Am J Cancer Res 2022;12(8):3811-3828
www.ajcr.us /ISSN:2156-6976/ajcr0143829

Original Article

A cellular senescence-related gene prognostic index for biochemical recurrence and drug resistance in patients with prostate cancer

Dechao Feng*, Xu Shi*, Jia You*, Qiao Xiong, Weizhen Zhu, Qiang Wei, Lu Yang

*Department of Urology, Institute of Urology, West China Hospital, Sichuan University, Chengdu 610041, Sichuan, People's Republic of China. *Equal contributors and co-first authors.*

Received April 29, 2022; Accepted July 12, 2022; Epub August 15, 2022; Published August 30, 2022

Abstract: In this study, we aimed to establish a novel cellular senescence-related gene prognostic index (CSG PI) to predict biochemical recurrence (BCR) and drug resistance in patients with prostate cancer (PCa) undergoing radical radiotherapy or prostatectomy. We performed all analyses using R version 3.6.3 and its suitable packages. Cytoscape 3.8.2 was used to establish a network of transcription factors and competing endogenous RNAs. Three cellular senescence-related genes were used to establish the CSGPI. We observed that CSGPI was an independent risk factor for BCR in PCa patients (HR: 2.62; 95% CI: 1.55-4.44), consistent with the results of external validation (HR: 1.88; 95% CI: 1.12-3.14). The CSGPI had a moderate diagnostic effect on drug resistance (AUC: 0.812, 95% CI: 0.586-1.000). The lncRNA PART1 was significantly associated with BCR (HR: 0.46; 95% CI: 0.27-0.77), and might modulate the mRNA expression of definitive genes through interactions with 57 miRNAs. Gene set enrichment analysis indicated that CSGPI was closely related to ECM receptor interaction, focal adhesion, TGF beta signaling pathway, pathway in cancer, regulation of actin cytoskeleton, and so on. Immune checkpoint analysis showed that PDCD1LG2 and CD96 were significantly higher in the BCR group compared to non-BCR group, and patients with higher expression of CD96 were more prone to BCR than their counterparts (HR: 1.79; 95% CI: 1.06-3.03). In addition, the CSGPI score was significantly associated with the mRNA expression of HAVCR2, CD96, and CD47. Analysis of mismatch repair and methyltransferase genes showed that DNMT3B was more highly expressed in the BCR group and that patients with higher expression of DNMT3B experienced a higher risk of BCR (HR: 2.08; 95% CI: 1.23-3.52). We observed that M1 macrophage, CD8+ T cells, stromal score, immune score, and ESTIMATE score were higher in the BCR group. In contrast, tumor purity was less scored in the BCR group. Spearman analysis revealed a positive relationship between CSGPI and M1 macrophages, CD4+ T cells, dendritic cells, stromal score, immune score, and ESTIMATE score. In conclusion, we found that the CSGPI might serve as a biomarker to predict BCR and drug resistance in PCa patients. Moreover, CD96 and DNMT3B might be potential treatment targets, and immune evasion might contribute to the BCR process of PCa.

Keywords: Cellular senescence, prostate cancer, tumor immune microenvironment, biochemical recurrence, immune checkpoint, methyltransferase

Introduction

Prostate cancer (PCa) is the second most common cancer and the sixth leading cause of cancer death worldwide [1]. Since the introduction of prostate specific antigen (PSA), 81% of new cases have been localized, and radical radiotherapy (RRT) and prostatectomy are two preferred treatments for these patients [2, 3]. Although the natural course of PCa is slow, among patients after radical therapy, the 15-year survival rate of those who suffer biochemical recurrence (BCR) within 3 years is 41% [4]. The impact of BCR on survival is believed to be limited to a subgroup of patients with specific clinical risk factors [5]. Nevertheless, BCR can promote the development of castration resistant prostate cancer (CRPC), and lead to an increased risk of long-term metastasis [5, 6]. In this case, clinicians are more concerned about how to predict high-risk groups of BCR and avoid overtreatment at the same time.

Senescence is a stable cell cycle arrest that occurs in both primary cells and cancer cells [7,

8]. Cell senescence may be a suboptimal response to anticancer therapies [9]. It is easy to understand that senescent cells can activate the immune system and promote the elimination of tumor cells, but it is worth noting that this activation is highly dependent on the tumor p53 status [10]. In prostate cancer, PTEN-deficient senescent tumors trigger highly immunosuppressive senescence-associated secretory phenotype (SASP) associated with increased infiltration of myeloid-derived suppressor cells [11]. Multiple studies have shown that senescent cells limit tumorigenesis and induce tumor progression, recurrence and metastasis of PCa at the late phase [12-15]. Furthermore, this two-sidedness of cellular senescence for cancer can be explained by the SASP of tumor cells, which refers to the model for explaining how senescent cells most likely promote senescence: the increased expression and secretion of inflammatory cytokines, chemokines, growth factors, and proteases [16]. However, the molecular and cellular mechanisms underlying cellular senescence and PCa are still poorly understood. In this study, we developed and validated a novel cellular senescence-related gene prognostic index (CSGPI) to predict biochemical recurrence (BCR) and drug resistance for patients with prostate cancer (PCa) undergoing radical radiotherapy or prostatectomy.

Methods

Data preparation

The training datasets were obtained from GSE46602 [17], GSE32571 [18], GSE62872 [19], and GSE116918 [20] after eliminating batch effects and the detailed process can be seen in our previous study [21]. We acquired the genes related to cellular senescence from GeneCards [22]. We used the TCGA database as the validation dataset. In addition, GSE42913 [23] was used to explore the diagnostic efficacy of CSGPI for drug resistance. Tumor related genes were considered as $|r| \geq 0.3$ and p.adj. < 0.0001 in weighted gene coexpression network analysis, and differentially expressed genes were regarded as $|logFC| \geq 0.4$ and p.adj. < 0.05.

Gene interaction, drug and cell line analysis

We analyzed the potential genes that might interact with definitive genes (ACACA, CTSB, and SERPINB5) using GeneMANIA [24]. We screened long noncoding RNAs (lncRNAs) associated with BCR-free survival and differentially expressed them between tumor and normal samples. Subsequently, we constructed a network of transcription factors (TFs) and competing endogenous RNAs (ceRNAs) using TRUST [25], lncBase [26], and miWalk [27]. We analyzed the drug sensitivity of definitive genes through GSCALite which included the data of the Cancer Therapeutics Response Portal (CTRP) [28], and the corporate cell lines of definitive genes was analyzed using canSAR [29].

Functional enrichment analysis

Gene Ontology (GO), including biological process (BP), cell composition (CC) and molecular function (MF), and Kyoto Encyclopedia of Genes and Genome (KEGG) analyses were conducted to explore the possible bioactivities and signaling pathways. We divided the 248 tumor patients undergoing RRT in GSE116918 [20] into high- and low-risk groups. We further conducted gene set enrichment analysis (GSEA) with "c2.cp.kegg.v7.4.symbols.gmt" and "h.all.v7.4.symbols.gmt" from the molecular signatures database [30]. We considered p.adj. < 0.05 and false discovery rate ≤ 0.25 were considered statistically significant.

Tumor immune microenvironment (TME) analysis

We explored the relationship between CSGPI and DNA mismatch repair (MMR) genes and methyltransferases using Spearman analysis [31]. The relationship between CSGPI and 20 common immune checkpoints was examined, as well as the differential expression between the BCR and non-BCR groups. We utilized the quanTiseq and ESTIMATE algorithms to score TME components [32-34]. Moreover, we conducted an analysis of differential expression, prognosis, and correlation for the above TME parameters and CSGPI score. **Figure 1** shows an overview of the procedures in this study.

Statistical analysis

We conducted all analyses using R software (version 3.6.3) and its suitable packages. Cytoscape 3.8.2 [35] was used to establish the TF-ceRNA network. We used the Wilcoxon test if the data did not satisfy a normal distribution.

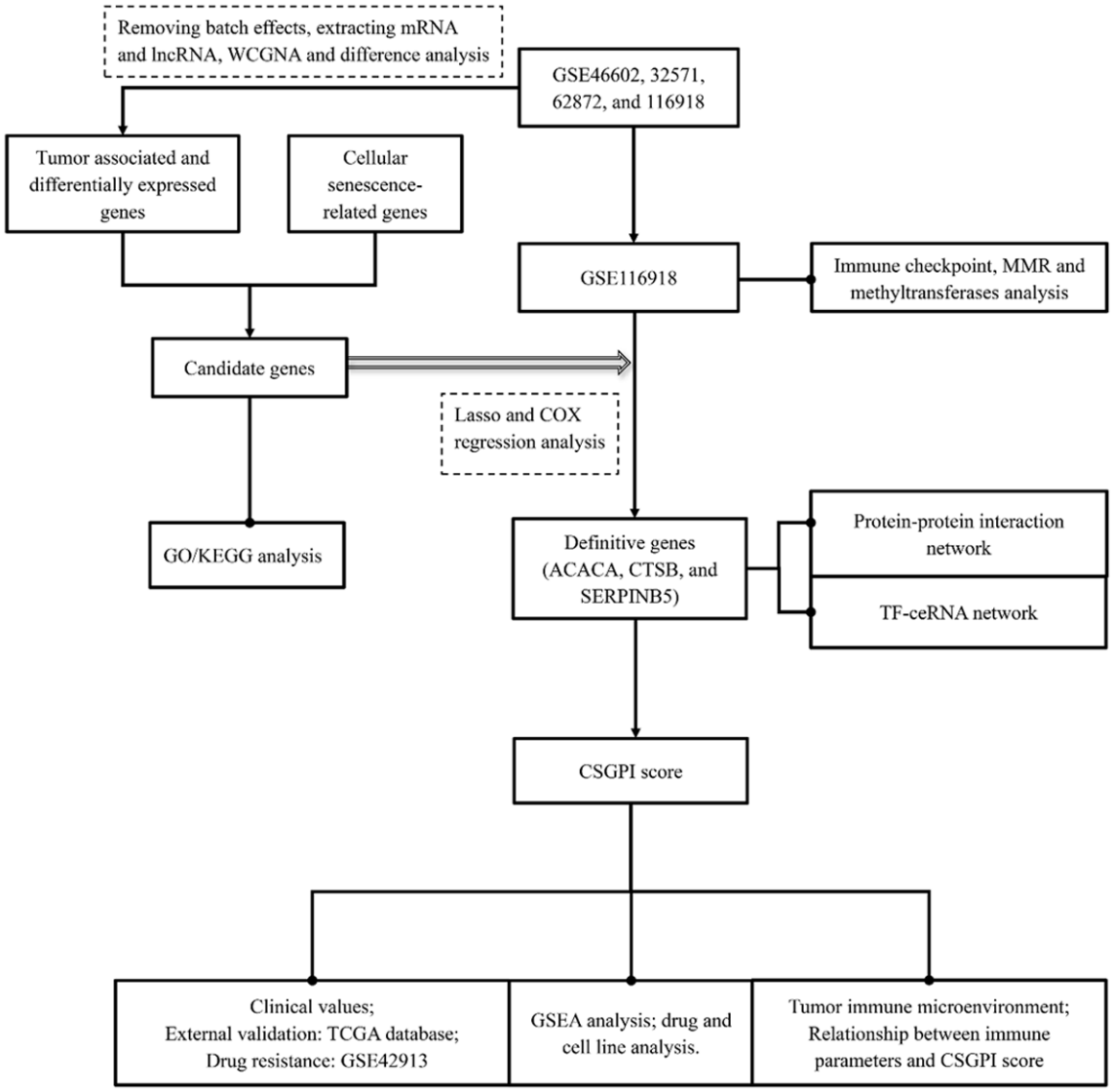

Figure 1. The detailed flowchart in this study. WGCNA = weighted gene coexpression network analysis; GO = gene ontology; KEGG = Kyoto Encyclopedia of Genes and Genome; GSEA = gene set enrichment analysis; TF = transcription factor; CSGPI = cellular senescence-related gene prognostic index; mRNA = message RNA; long noncoding RNA = lncRNA.

Variables were enrolled in the multivariate Cox regression analysis if the *p* value < 0.1 in the univariable Cox regression analysis. Statistical significance was set as two-sided P < 0.05. Significance was marked as follows: ns, P ≥ 0.05; *, P < 0.05; **, P < 0.01; ***, P < 0.001.

Results

CSGPI score and prognostic values

We eventually determined ACACA, CTSB, and SERPINB5 to be definitive genes after intersection of tumor-related genes, differentially expressed genes, and genes associated with BCR free survival, and Lasso and COX regression analysis (**Figure 2A-F**). These genes could discriminate high-risk patients from low-risk patients (**Figure 2G**). The risk score based on ACACA, CTSB, and SERPINB5 was CSGPI score =-0.88714*ACACA + 0.97560*CTSB - 1.79755*SERPINB5. The CSGPI was highly positively correlated with PSA (r: 0.652, P= 0.029; **Figure 2H**). We observed moderate diagnostic accuracy of the CSGPI score distinguishing BCR from no BCR stably (AUCs were

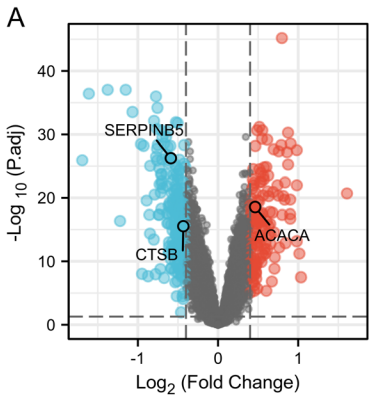

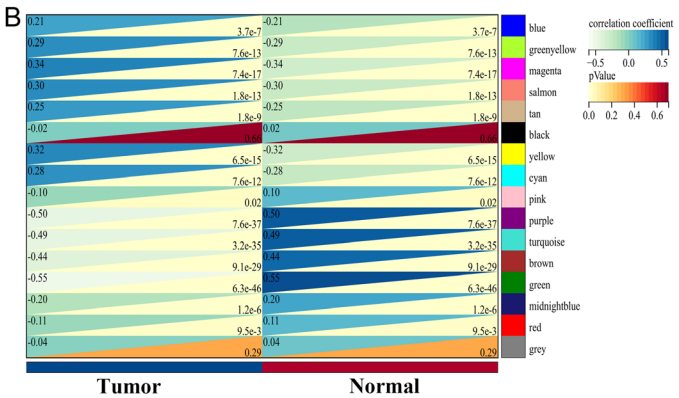

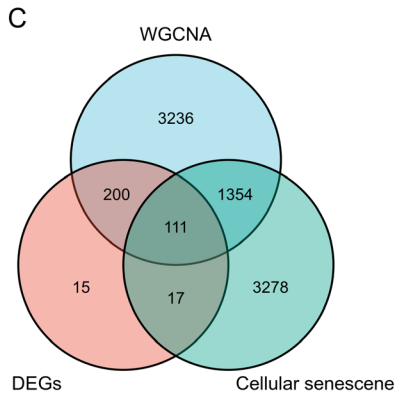

D

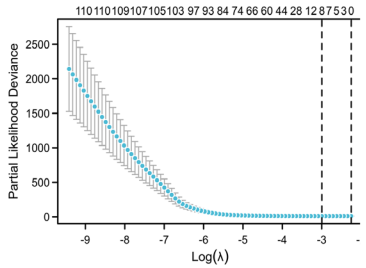

E

Genes	Hazard ratio (95% CI)	P value
Univariate analysis		
ACACA	0.476 (0.233-0.976)	0.043
ALDH2	0.571 (0.415-0.785)	<0.001
CTSB	2.349 (1.079-5.112)	0.031
IGF1	0.516 (0.351-0.756)	<0.001
KRT15	0.744 (0.629-0.880)	<0.001
PTN	0.447 (0.273-0.730)	0.001
SERPINB5	0.299 (0.092-0.975)	0.045
SPP1	1.378 (1.132-1.677)	0.001
Multivariate analysis		
ACACA	0.412 (0.188-0.900)	0.026
ALDH2	0.740 (0.478-1.145)	0.176
CTSB	2.653 (1.047-6.721)	0.04
IGF1	0.831 (0.505-1.365)	0.464
KRT15	0.863 (0.697-1.070)	0.18
PTN	0.701 (0.411-1.196)	0.192
SERPINB5	0.166 (0.040-0.692)	0.014
SPP1	1.214 (0.953-1.547)	0.116

F

Characteristics	Hazard ratio (95% CI)	P value
Univariate analysis		
CSGPI score		
Low	Reference	
High	2.630 (1.488-4.650)	<0.001
Age		
≤ 60	Reference	
> 60	0.809 (0.408-1.604)	0.544
T stage		
T1	Reference	
T2	1.504 (0.577-3.917)	0.404
T3	2.599 (1.075-6.282)	0.034
T4	11.987 (2.963-48.501)	<0.001
Gleason score		
G6	Reference	
G7	1.876 (0.760-4.632)	0.173
G8	2.031 (0.771-5.346)	0.151
G9	2.458 (0.951-6.355)	0.064
Multivariate analysis		
CSGPI score		
Low	Reference	
High	2.735 (1.495-5.003)	0.001
T stage		
T1	Reference	
T2	1.623 (0.622-4.231)	0.322
T3	2.757 (1.139-6.671)	0.025
T4	11.966 (2.940-48.697)	<0.001

G

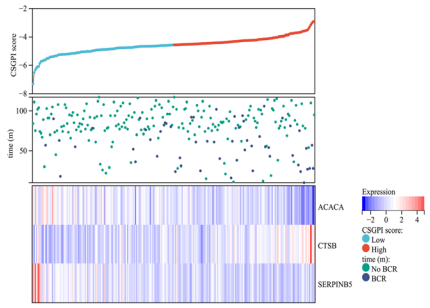

H

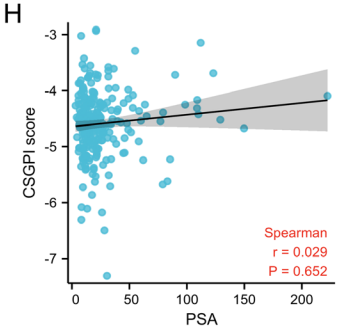

I

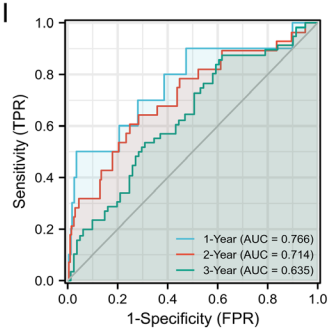

J

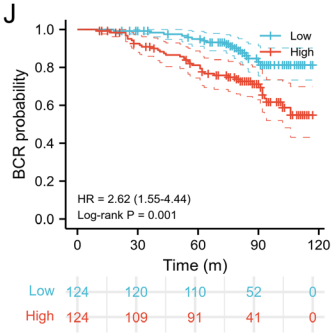

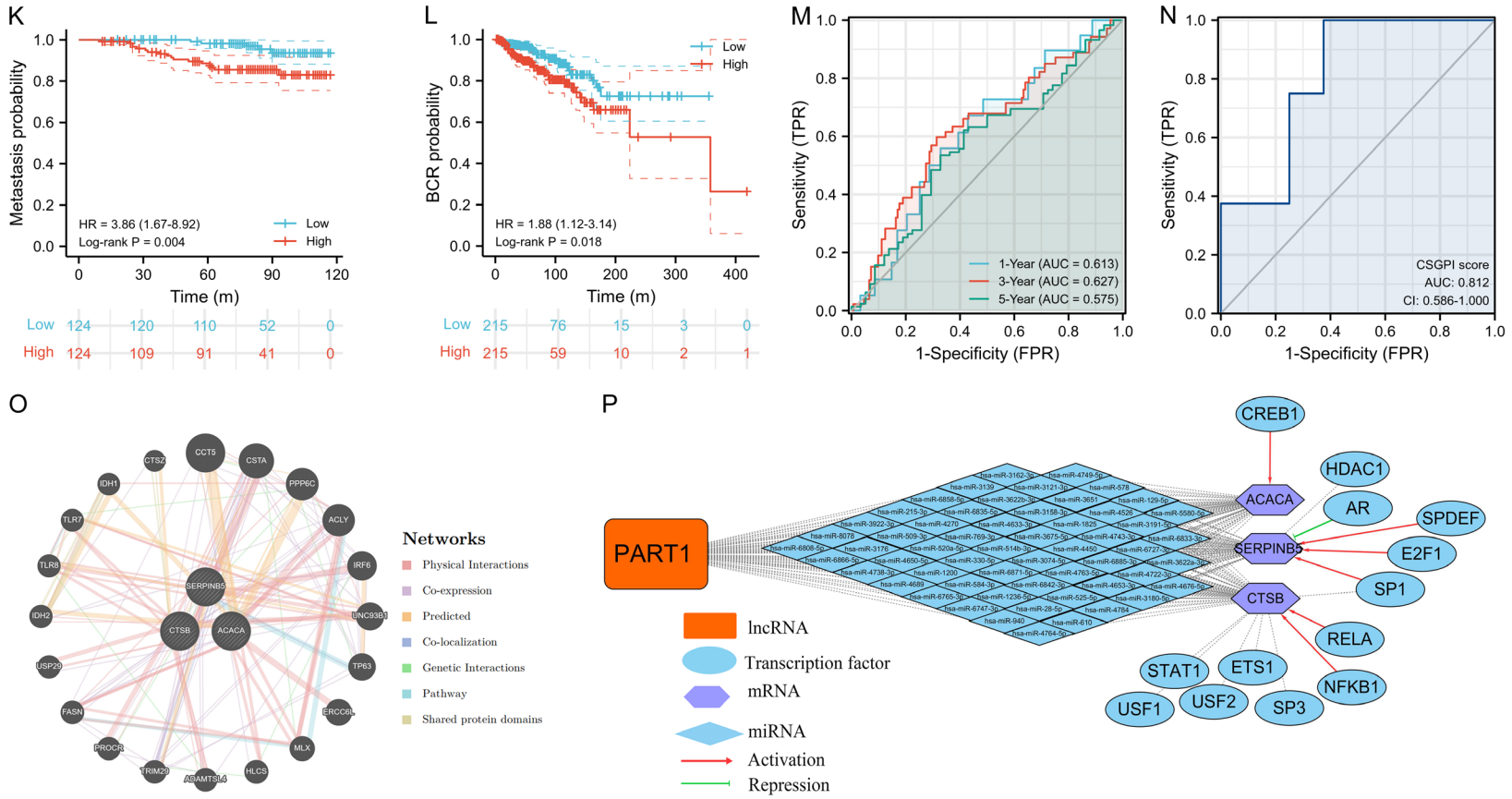

Figure 2. Process of screening definitive genes and clinical values. A. Volcano plot showing the mRNA expression of definitive genes between tumor and normal tissues; B. Modules and phenotype showing the tumor-related modules; C. Venn plot showing DEGs associated with tumor and cellular senescence; D. Gene screening through Lasso regression; E. Genes associated with BCR-free survival in PCa using univariate and multivariate COX analysis after Lasso regression; F. Examining the clinical values of CSGPI score using univariate and multivariate COX analysis for BCR free survival; G. Plot of risk factor showing the distribution of high- and low-risk patients; H. Correlation between CSGPI score and PSA; I. Time dependent ROC curve of CSGPI score discriminating BCR from no BCR; J. Kaplan-Meier curve showing survival differences between high- and low-risk patients for BCR free survival; K. Kaplan-Meier curve showing survival differences between high- and low-risk patients for metastasis free survival; L. External validation of CSGPI score through Kaplan-Meier curve showing survival differences between high- and low-risk patients for BCR free survival in TCGA dataset; M. Time dependent ROC curve of CSGPI score discriminating BCR from no BCR in TCGA dataset; N. ROC curve showing the diagnostic ability of CSGPI for drug chemoresistance; O. Protein-protein network of ACACA, CTSB, and SERPINB5; P. TF-ceRNA network of ACACA, CTSB, and SERPINB5. CSGPI = cellular senescence-related gene prognostic index; ROC = receiver operating characteristic; BCR = biochemical recurrence; PSA = prostate specific antigen; TF = transcription factor; ceRNA = competing endogenous RNA; PCa = prostate cancer.

0.766, 0.714, and 0.635 for 1 year, 2 years, and 3 years, respectively; **Figure 2I**). In GSE116918 [20], patients in the high-risk group had higher risk of BCR (HR: 2.62, 95% CI: 1.55-4.44, P=0.001) and metastasis (HR: 3.86, 95% CI: 1.67-8.92, p=0.004) than those in the low-risk group (**Figure 2J**, **2K**). We observed similar results in the TCGA dataset for BCR-free survival (HR: 1.88, 95% CI: 1.12-3.14, P=0.018; **Figure 2L**) and diagnostic accuracy (AUCs were 0.613, 0.627, and 0.575 for 1 year, 2 years, and 3 years, respectively; **Figure 2M**). For drug resistance, the diagnostic accuracy was 0.812 (95% CI: 0.586-1.000; **Figure 2N**). The possible genes that interacted with ACACA, CTSB, and SERPINB5 included CCT5, CSTA, PPP6C, ACLY, IRF6, UNC93B1, TP63, ERCC6L, MLX, HLCS, ADAMTSL4, TRIM29, PROCR, FASN, USP29, IDH2, TLR8, TLR7, IDH1, and CTSZ (**Figure 2O**). We detected that patients expressing higher lncRNA PART1 had a lower risk of BCR than their counterpart (HR: 0.46, 95% CI: 0.27-0.77, P=0.004; not shown). We subsequently constructed the ceRNA network. PART1 might regulate the expression of ACACA, CTSB, and SERPINB5 through 57 common miRNAs (**Figure 2P**). In addition, TFs including SPDEF, E2F1, SP1, CREB1, RELA, and NFKB1, could activate the expression of ACACA, CTSB, and SERPINB5, while AR could repress the expression of SERPINB5 (**Figure 2P**). Overall, **Figure 2** shows the process of screening definitive genes, clinical values of CSGPI scores, possibly interacting genes and the regulatory network of definitive genes.

Functional enrichment analysis

Figure 3 presents the GO functions of the candidate genes. BP analysis indicated that candidate genes were mainly involved in cell junction assembly and organization, reproductive structure and system development, gland development, and regulation of epithelial cell proliferation (**Figure 3A**). CC analysis showed that candidate genes were mainly involved in collagen-containing extracellular matrix (ECM), contractile fiber, I band, myofibril, sarcomere, Z disc, and focal adhesion (**Figure 3B**). MF analysis showed that candidate genes mainly participated in actin binding, extracellular matrix binding, cell adhesion mediator activity, structural constituent of cytoskeleton, cadherin binding involved in cell-cell adhesion, and integrin binding (**Figure 3C**). KEGG analysis indicated that candidate genes were mainly involved in focal adhesion, proteoglycans in cancer, glutathione metabolism, TGF-beta and Wnt and MAPK signaling pathways, platinum drug resistance, and pyruvate metabolism (**Figure 3D**). **Figure 4** shows the GSEA results of high- and low-risk patients. GSEA showed that high-risk patients were enriched in ECM receptor interaction, focal adhesion, TGF-beta signaling pathway, regulation of actin cytoskeleton, NOD like receptor signaling pathway, FC gamma-R mediated phagocytosis, chemokine signaling pathway, apoptosis, complement and coagulation cascades, intestinal immune network for IGA production, lysosome, Wnt signaling pathway, adhesion junction, P53 signaling pathway, GAP junction, and cytokine-cytokine receptor interaction (**Figure 4A**).

TME, drug, and cell line analysis

We observed that PDCD1LG2 (P=0.038) and CD96 (p=0.013) were expressed at higher levels in the BCR group than in the non-BCR group (**Figure 5A**), and higher expression of CD96 was associated with a higher risk of BCR (HR: 1.79, 95% CI: 1.06-3.03, P=0.032; **Figure 5B**). Spearman analysis showed that the CSGPI score was significantly associated with the mRNA expression of HAVCR2 (r: 0.29, P < 0.001), CD96 (r: 0.15, P=0.016), CD47 (r: 0.16, P=0.012), and LAG3 (r: -0.15, P=0.018) (**Figure 5C**). DNMT3B was expressed at higher levels in the BCR group (**Figure 5D**) and was closely associated with BCR free survival (HR: 2.08, 95% CI: 1.23-3.52, P=0.008; **Figure 5E**). Moreover, we observed that M1 macrophages (P=0.022), CD8+ T cells (P=0.016), stromal score (P=0.003), immune score (P=0.012), and estimate score (P=0.003) had higher scores in the BCR group than in the non-BCR group (**Figure 5F**, **5G**). However, the tumor purity showed a opposite difference (P=0.003, **Figure 5G**). We found that the CSGPI score was significantly related to M1 macrophages (r: 0.35), M2 macrophages (r: -0.31), neutrophils (r: -0.13), CD4+ T cells (r: 0.2), dendritic cells (r: 0.26), stromal score (r: 0.49), immune score (r: 0.45), estimate score (r: 0.49), and tumor purity (r: -0.49) (**Figure 5H**). For drug analysis, we found that 24 drugs might be sensitive to ACACA, CTSB, and SERPINB5 (**Figure 5I**), among which the top 10 drugs were 1S, 3R-RSL-3, CIL70, ML162, ML210, PI-103, PYR-41, UNC0638, bendamustine, manumycin A, and sunitinib (**Figure 5J**).

A

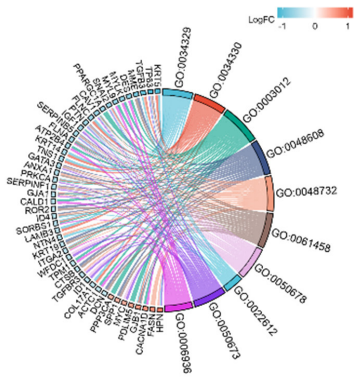

Ontology	ID	Description	GeneRatio	BgRatio	p.adjust	qvalue
BP	GO:0034329	cell junction assembly	14/111	241/18670	2.79e-07	2.01e-07
BP	GO:0034330	cell junction organization	15/111	290/18670	2.79e-07	2.01e-07
BP	GO:0003012	muscle system process	18/111	465/18670	2.80e-07	2.02e-07
BP	GO:0048608	reproductive structure development	16/111	431/18670	3.01e-06	2.17e-06
BP	GO:0048732	gland development	16/111	434/18670	3.01e-06	2.17e-06
BP	GO:0061458	reproductive system development	16/111	434/18670	3.01e-06	2.17e-06
BP	GO:0050678	regulation of epithelial cell proliferation	15/111	378/18670	3.01e-06	2.17e-06
BP	GO:0022612	gland morphogenesis	9/111	120/18670	1.47e-05	1.06e-05
BP	GO:0050673	epithelial cell proliferation	15/111	434/18670	1.47e-05	1.06e-05
BP	GO:0006936	muscle contraction	13/111	360/18670	6.81e-05	4.91e-05

B

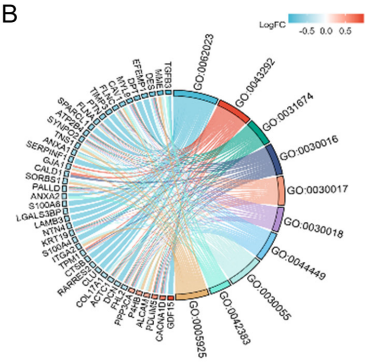

Ontology	ID	Description	GeneRatio	BgRatio	p.adjust	qvalue
CC	GO:0062023	collagen-containing extracellular matrix	20/111	406/19717	2.89e-11	2.12e-11
CC	GO:0043292	contractile fiber	16/111	234/19717	3.53e-11	2.59e-11
CC	GO:0031674	I band	13/111	143/19717	1.22e-10	8.97e-11
CC	GO:0030016	myofibril	15/111	224/19717	1.40e-10	1.02e-10
CC	GO:0030017	sarcomere	14/111	204/19717	4.56e-10	3.34e-10
CC	GO:0030018	Z disc	12/111	132/19717	4.64e-10	3.40e-10
CC	GO:0044449	contractile fiber part	14/111	221/19717	9.56e-10	7.01e-10
CC	GO:0030055	cell-substrate junction	16/111	412/19717	4.18e-08	3.07e-08
CC	GO:0042383	sarcolemma	10/111	136/19717	1.41e-07	1.03e-07
CC	GO:0005925	focal adhesion	15/111	405/19717	2.17e-07	1.59e-07

C

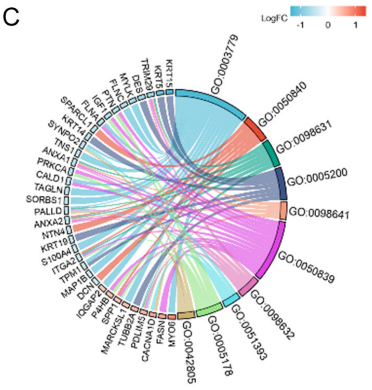

Ontology	ID	Description	Gene Ratio	BgRatio	p.adjust	qvalue
MF	GO:0003779	actin binding	16/110	431/17697	3.30e-06	2.70e-06
MF	GO:0050840	extracellular matrix binding	6/110	57/17697	1.91e-04	1.56e-04
MF	GO:0098631	cell adhesion mediator activity	6/110	59/17697	1.91e-04	1.56e-04
MF	GO:0005200	structural constituent of cytoskeleton	7/110	102/17697	2.78e-04	2.27e-04
MF	GO:0098641	cadherin binding involved in cell-cell adhesion	4/110	19/17697	3.37e-04	2.76e-04
MF	GO:0050839	cell adhesion molecule binding	13/110	499/17697	6.79e-04	5.55e-04
MF	GO:0098632	cell-cell adhesion mediator activity	5/110	50/17697	6.79e-04	5.55e-04
MF	GO:0051393	alpha-actinin binding	4/110	37/17697	0.003	0.003
MF	GO:0005178	integrin binding	6/110	132/17697	0.006	0.005
MF	GO:0042805	actinin binding	4/110	46/17697	0.006	0.005

D

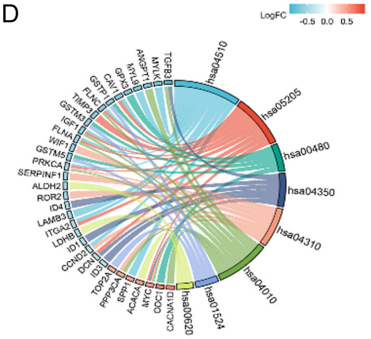

Ontology	ID	Description	GeneRatio	BgRatio	p.adjust	qvalue
KEGG	hsa04510	Focal adhesion	11/74	201/8076	3.70e-04	3.05e-04
KEGG	hsa05205	Proteoglycans in cancer	9/74	205/8076	0.005	0.004
KEGG	hsa00480	Glutathione metabolism	5/74	57/8076	0.007	0.005
KEGG	hsa04350	TGF-beta signaling pathway	6/74	94/8076	0.007	0.006
KEGG	hsa04310	Wnt signaling pathway	7/74	160/8076	0.018	0.015
KEGG	hsa04010	MAPK signaling pathway	9/74	294/8076	0.035	0.029
KEGG	hsa01524	Platinum drug resistance	4/74	73/8076	0.089	0.073
KEGG	hsa00620	Pyruvate metabolism	3/74	39/8076	0.090	0.074

Figure 3. Gene ontology analysis of candidate genes. A. BP analysis; B. CC analysis; C. MF analysis; D. KEGG analysis; KEGG = Kyoto Encyclopedia of Genes and Genome; BP = biological process; CC = cell composition; MF = molecular function.

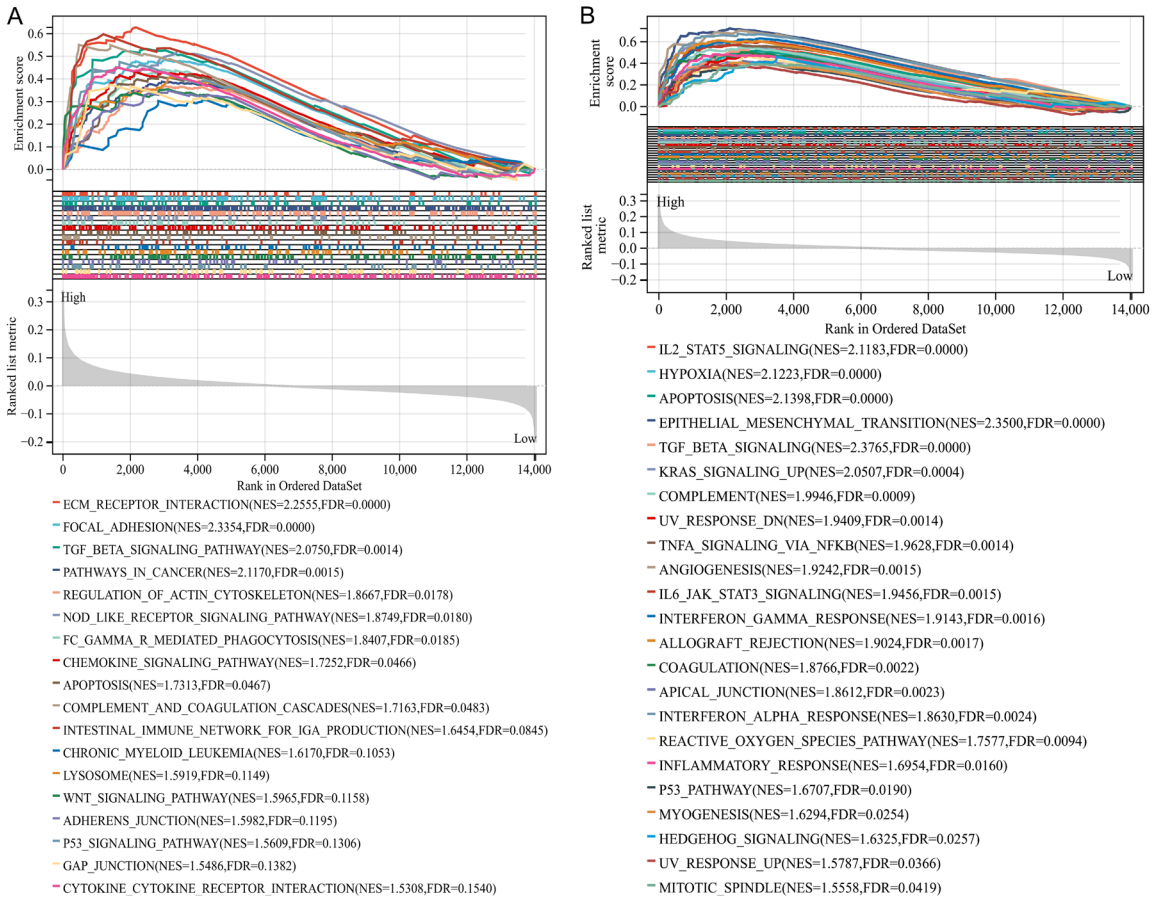

Figure 4. GSEA analysis of high- and low-risk patients with prostate cancer. A. GSEA C2 analysis; B. GSEA hallmark analysis; GSEA = gene set enrichment analysis. Prostate cancer patients were divided into high- and low-risk groups according to the median value of the cellular senescence-related gene prognostic index.

The cell line analysis indicated that PRECLH, DU145, PC3, MDAPCA2B, 22RV1, NCIH660, and VCAP were potential cell lines to investigate CTSB, ACACA, and SERPINB5 in PCa (**Figure 5K**). Overall, **Figure 5** shows the analyses of TME, MMR, methyltransferase genes, drug and potential cell lines in PCa patients.

Discussion

For low- and intermediate-risk localized prostate cancer, RRT is as effective as radical prostatectomy (RRP) [36]. However, for the high-risk subgroup, the risk of recurrence after RRT is increased [37]. After treatment and cure of PCa, some patients may have disease recurrence confirmed by PSA blood tests, namely BCR. However, not everyone who experiences BCR will develop a progressive disease [38]. Despite the development of the diagnosis and treatment of PCa during the past few decades, the survival rate of patients has often improved by meager months [39]. The development of models that predict BCR can help optimize decision-making strategies for PCa management.

Cellular senescence is a complex stress response, accompanied by a large number of changes in gene expression [40]. Senescence can be induced by cancer chemotherapy drugs and radiation, known as therapy-induced senescence (TIS) [9, 41]. What needs to be clear is that tumor cells in vitro and in vivo have been found to escape from TIS, accompanied by a reduction in the expression of select SASP components [42, 43]. In other words, senescent tumor cells can actually re-enter the cell cycle after senescence, and these cells acquire stem cell-like characteristics, which may represent a possibility of recurrence [44-46]. Demaria et al. found that senescent nontumor cells are conducive to cancer recurrence and metastasis after chemotherapy in a murine

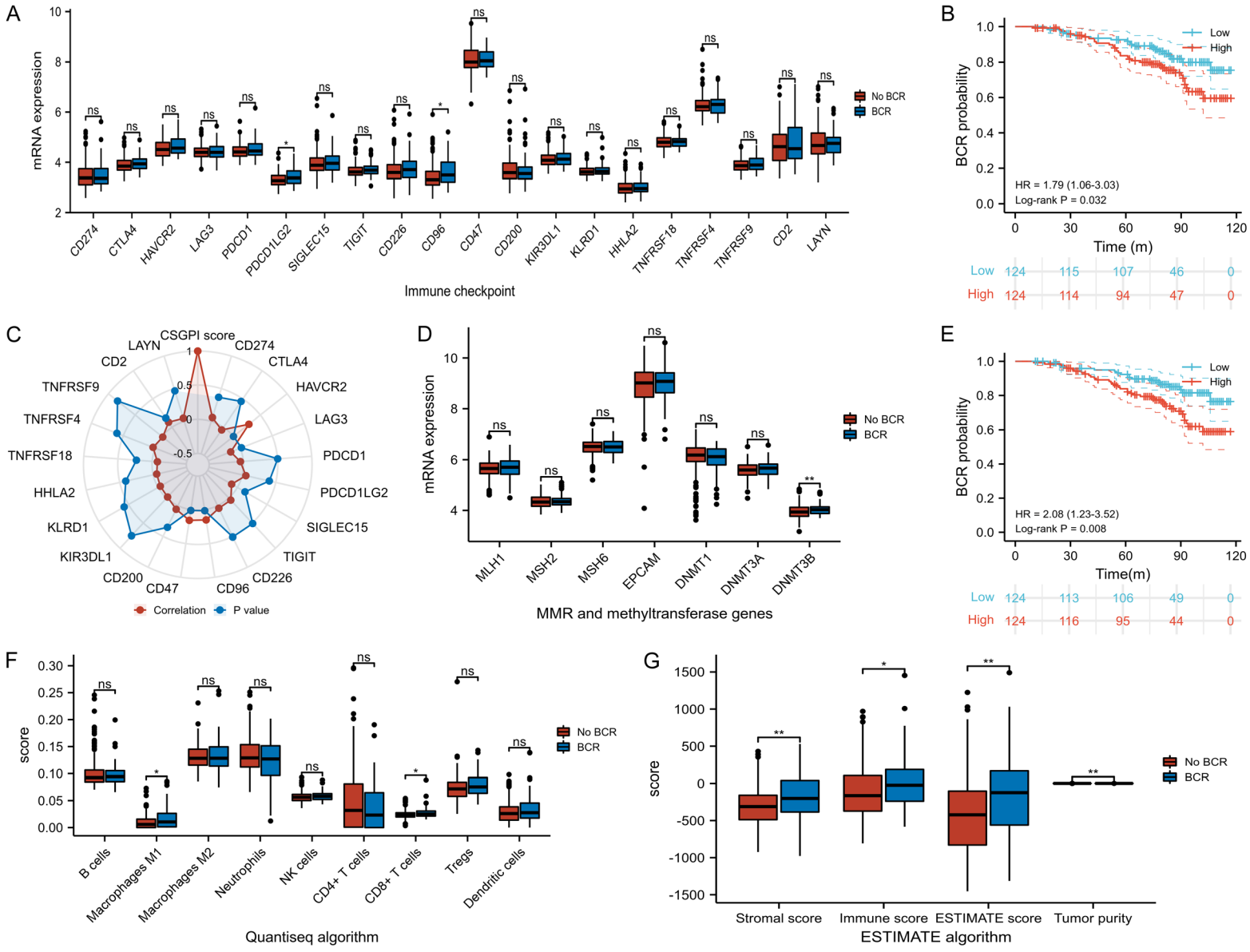
A
mRNA expression
Immune checkpoint
CD274
CTLA4
HAVCR2
LAG3
PDCD1
PDCD1LG2
SIGLEC15
TIGIT
CD226
CD96
CD47
CD200
KIR3DL1
KLRD1
HHLA2
TNFRSF18
TNFRSF4
TNFRSF9
CD2
LAYN
No BCR
BCR
B
BCR probability
HR = 1.79 (1.06-3.03)
Log-rank P = 0.032
Time (m)
Low 124 115 107 46 0
High 124 114 94 47 0
C
CSGPI score
Correlation
P value
D
mRNA expression
MMR and methyltransferase genes
MLH1
MSH2
MSH6
EPCAM
DNMT1
DNMT3A
DNMT3B
E
BCR probability
HR = 2.08 (1.23-3.52)
Log-rank P = 0.008
Time(m)
Low 124 113 106 49 0
High 124 116 95 44 0
F
score
Quantiseq algorithm
B cells
Macrophages M1
Macrophages M2
Neutrophils
NK cells
CD4+ T cells
CD8+ T cells
Tregs
Dendritic cells
G
score
ESTIMATE algorithm
Stromal score
Immune score
ESTIMATE score
Tumor purity

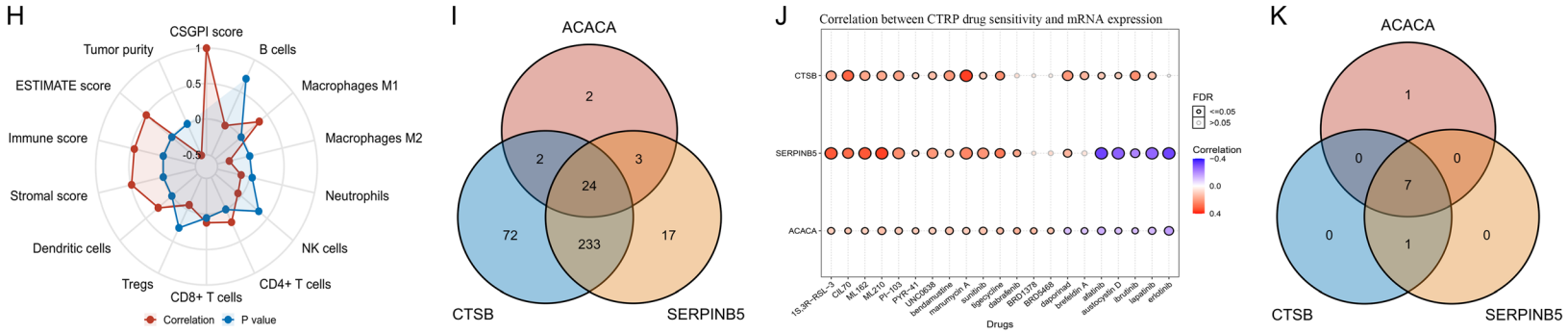

Figure 5. TME, drug, and cell line analysis. A. Comparison between BCR and no BCR group for immune checkpoints; B. Kaplan-Meier curve showing survival differences of high- and low-expression of CD96 for BCR free survival; C. Radar plot showing correlation between immune checkpoints and CSGPI score; D. Comparison between BCR and no BCR group for mismatch repair and methyltransferase genes; E. Kaplan-Meier curve showing survival differences of high- and low-expression of DNMT3B for BCR free survival; F. Comparison between BCR and no BCR group for TME cells; G. Comparison between BCR and no BCR group for TME score; H. Radar plot showing correlation TME parameters and CSGPI score; I. Venn plot showing common sensitive drugs of ACACA, CTSB, and SERPINB5 through the CTRP database; J. Plot showing the top 30 potential drugs for ACACA, CTSB, and SERPINB5 through the CTRP database; K. Venn plot showing common cell lines of ACACA, CTSB, and SERPINB5 in prostate cancer. TME = tumor immune microenvironment; CSGPI = cellular senescence-related gene prognostic index; BCR = biochemical recurrence; CTRP = the cancer therapeutics response portal.

model [14]. Milanovic et al. found that senescence-associated reprogrammed cells, with stemness, were found to have much higher tumor initiation potential than virtually identical cells and is enriched in relapsed tumors, which may have a long-term impact on tumor aggressiveness and prognosis for leukemia [16]. The elimination of senescent cells after doxorubicin treatment can improve inflammation and tumor recurrence through cell-autonomous mechanisms as well as paracrine signaling through the SASP. SASP factors are involved in the recruitment of natural killer cells (NK) and macrophages and the "reprogramming" of macrophages to the tumor-inhibiting M1 phenotype [47, 48].

Moreover, SASP has been shown to induce epithelial-mesenchymal transition (EMT), thereby increasing invasiveness [49-52]. However, for PCa, the presence of senescent cells only increased the proliferation of cocultured cells in vitro but did not significantly change tumor growth in vivo, which indicates negligible proliferative bystander effects of senescent PCa cells that depend on the expression of SASP components in the TME [47, 53]. In fact, SASP is now divided into those derived from acute senescent cells (A-SASP) and chronic senescent cells (C-SASP), among which A-SASP is more effective in inducing the senescence of immortalized prostate cells [54, 55]. Recent studies have shown that SASP induced senescence of immortalized prostate cells but not of metastatic PCa cells in vitro, suggesting that acute senescent cells only act to resist tumorigenesis rather than directly fight against malignant cells [56]. Borrowing this theory can partly explain how senescent cells mediate two opposite effects of tumor suppression and promotion [57, 58]. Recently, Tonnessen-Murray et al. found that chemotherapy-induced senescent cancer cells often engulf adjacent senescent or nonsenescent tumor cells at a significant frequency to gain a survival advantage, leading to breast cancer recurrence and poor prognosis [59]. We speculated that a similar mechanism might exist for PCa cells after receiving RRT, since adherent senescent-like cells expressing common senescence-associated markers resulted in generation among several prostate cancer cell lines after ionizing radiation [60]. The mechanism may involve miR-106a, which can confer radiation resistance by reducing senescence [61].

The expression of lncRNA PART1 was found to be related to the poor prognosis and tumor recurrence of stage I-III non-small cell lung cancer and hepatocellular carcinoma [62-64]. SERPINB5, as a gene related to cancer cell motility, is believed to contribute to tumor invasion, migration and final metastasis [65]. Zhang et al. found that the ubiquitination of guanine monophosphate synthase (GMPS) mediated by SERPINB5 promotes TP53 inhibition, resulting in radiation resistance in nasopharyngeal carcinoma cells, which may help us understand that SERPINB5 may also be involved in the survival promotion and recurrence of PCa cells after RRT [66]. Here, we demonstrated for the first time the ability of the expression of lncRNA PART1 and its regulated mRNA to predict BCR and drug resistance after RRT in PCa. In addition, the CSGPI score based on in this study could predict BCR free survival for PCa patients undergoing RRP.

The senescence bystander effect mentioned above refers to the phenomenon that senescent cells cause the development of senescent phenotype in nearby cells [67]. This effect was found to be related to thrombospondin-1-dependent activation of the TGF-β1 signaling pathway through ROS and their downstream effector, p38 MAPK [68, 69]. The TGF-β1 signaling pathway is related to premature senescence of human diploid fibroblasts (HDFs) [70, 71]. Furthermore, inhibition of the TGF-β1 signaling pathway was found to prevent mouse primary prostate fibroblasts from radiation-induced damage, which means, from another perspective, radiation resistance and the subsequent recurrence of PCa [72]. This is consistent with the results of our gene set enrichment analysis. The possible speculation is that the oxidative stress and the subsequent cell senescence caused by the TGF beta signaling pathway led to the bystander effect of the tumor and its surrounding counterparts in PCa tissue thus promoting the occurrence of BCR. ECM receptor interaction and focal adhesion are two other mechanisms that may link cell senescence with BCR. The ECM is a component of the TME that affects the biological behavior of PCa and mediates cell differentiation, migration and invasion [73, 74]. Lichner et al. found that miR-29c, miR-34a and miR-141 are differentially expressed in different Gleason grades, and their main biological processes include ECM-mediated signaling and focal

adhesion kinase- and mitogen-activated kinase pathways, with miR-29c and miR-34a influencing downstream pathways that affect actin cytoskeleton organization [75]. Furthermore, miR-29c, miR-34a, miR-141 and miR-148a showed inverse correlations with BCR [75].

The high expression level of PDCD1LG2 has been found to be associated with a worse BCR free survival for PCa [76]. PDCD1LG2 was found to be related to immunomodulatory and radiation response pathways, suggesting its role in predicting prognosis and response to treatment as a promising immune checkpoint target [76]. In our study, we found higher expression of PDCD1LG2 in the BCR group, but an association with BCR-free survival was not observed. The DNA methyltransferase DNMT3B is highly abundant in several prostate cancer cell lines. By targeting RAD9 to methylate, it regulates tumorigenicity, castration resistance, androgen-independent growth and metastasis of PCa [77, 78]. Moreover, DNMT3B mRNA expression is associated with an increased cancer aggressiveness and risk of lethal PCa [79]. Combined with our research, it is also suggested that DNA methylation may be related to the occurrence of BCR.

The TME is a collection of tumor cells and quiet nontumor cells [80]. A large number of studies have shown that the TME is involved in tumor progression and response to treatment by nourishing the tumor parenchyma [81, 82]. In the TME, macrophages play an important regulatory function [83]. Classically activated macrophages in TME (M1 macrophages, CD14++ CD16-) show antitumor activity, while alternatively activated macrophages (M2 macrophages, CD14+ CD16++) possess anti-inflammatory functions and promote wound healing, angiogenesis and tissue remodeling, thereby supporting tumor progression and metastasis [84]. The polarization of macrophages in particular depends on SASP in the TME [85]. As mentioned above, p53-dependent senescent hepatic stellate cells (HSCs) release specific SASP factors including IFN-γ and IL-6, which bias the polarization of macrophages in favor of the M1 state, while proliferating p53-deficient HSCs promote the conversion of macrophages to the M2 phenotype through IL-4 [10]. Di Mitri et al. found that PTEN-null PCa tissue, which is vulnerable to TNF-α-induced senescence, was strongly infiltrated by macrophages and promoted the polarization of macrophages to the TNF-α-secreting M1 phenotype through CXCR2 [86]. Senescence establishes the antitumor TME through SASP, which regulates the function of macrophages, and inhibits the tumorigenesis of neighboring cells in a noncell-autonomous manner [48]. Most tumor-associated macrophages (TAMs) have the M1 phenotype, and TAMs can induce senescence and tumor inhibition [86, 87]. Combined with the results of our analysis, it is further confirmed that senescent PCa cells, such as HSCs, can promote the transformation of macrophages from the M2 to the antitumor M1 phenotype through SASP. Here we suggest the therapeutic effect of macrophage-targeting therapy in PCa, such as the application of an α-CSF-1R monoclonal antibody for colorectal adenocarcinoma and fibrosarcoma [88].

Senescent cells undergo immune surveillance from T cells through adaptive immunity as well. Various SASP factors including CCL27, CCL2, CXCL11 and IL-1α are related to the mobilization, activation and differentiation of T cells [89, 90]. The potential recruitment of activated T lymphocyte subsets to sites occupied by senescent cells has been witnessed [49, 90-92]. The activation, differentiation and functional specialization of T cells are finely regulated [93]. The CD4+ T-cell response as a Th1 type response, rather than direct T cell cytotoxicity, effectively kills precancerous senescent hepatocytes [92]. The percentage of stromal cells in the TME represents the stromal score [94]. In all solid tumors, abundant matrix often represents a worse prognosis, with deeper invasion depth and lymph node metastasis probability [95]. The prostate stroma is an important component for normal prostate growth and differentiation, compared with PCa, where the increase in collagen fibers and carcinoma-associated fibroblasts (CAFs) accompanied a decrease in smooth muscle cells as cancer progresses [96]. This change in stroma is similar to wound healing and is called 'reactive stroma' [97-99]. Reactive matrix grading (RSG) has been a tool to assess PCa-specific mortality in diagnostic prostate needle biopsies [100]. In univariate analysis, level 3 RSG can predict the time and risk of biochemical recurrence after radical prostatectomy [101]. Moreover, CD96 was expressed on T cells and NK cells together with CD226 and TIGIT, contributing to tumor escape from the immune system [102]. Thus, we proposed that immune

evasion played a vital role in the BCR process of PCa.

Here, we identified genes and pathways related to cellular senescence and BCR in PCa, and built a CSGPI risk score to predict BCR and drug resistance. Behind this score, we also revealed that the occurrence of BCR may be related to various immune cells and SASP in the TME. In summary, senescence is a specific response of cancer cells to antitumor treatments including RRT. Combined with research results in other cancers, we speculated that senescent cells might play a major role in promoting BCR after RRT in the short term through the reversible process of TIS and SASP in the TME. However, for the subsequent treatment of prostate cancer, senescence induction remains a potential treatment method through activation of the immune system. Indeed, we have to admit that most of the findings, such as the ceRNA network and the potential targets identified in this study, warrant further investigation.

Conclusion

We found that the CSGPI might serve as a biomarker to predict BCR and drug resistance in PCa patients. Moreover, CD96 and DNMT3B might be potential treatment targets, and immune evasion might contribute to the BCR process of PCa.

Acknowledgements

The results showed here are in whole or part based upon data generated by the TCGA Research Network: https://www.cancer.gov/tcga. This program was supported by the National Natural Science Foundation of China (Grant Nos. 81974099, 82170785, 81974098, 82170784), programs from Science and Technology Department of Sichuan Province (Grant No. 2021YFH0172), Young Investigator Award of Sichuan University 2017 (Grant No. 2017SCU04A17), Technology Innovation Research and Development Project of Chengdu Science and Technology Bureau (2019-YF05-00296-SN), Sichuan University-Panzhihua science and technology cooperation special fund (2020CDPZH-4). The funders had no role in the study design, data collection or analysis, preparation of the manuscript, or the decision to publish.

Disclosure of conflict of interest

None.

Address correspondence to: Qiang Wei and Lu Yang, Department of Urology, Institute of Urology, West China Hospital, Sichuan University, Guoxue Xiang #37, Chengdu 610041, Sichuan, People's Republic of China. Tel: +86-28-85422444; Fax: +86-28-85422451; E-mail: weiqiang933@126.com (QW); wycleflue@scu.edu.cn (LY)

References

[1] Center MM, Jemal A, Lortet-Tieulent J, Ward E, Ferlay J, Brawley O and Bray F. International variation in prostate cancer incidence and mortality rates. Eur Urol 2012; 61: 1079-92.

[2] Newcomer LM, Stanford JL, Blumenstein BA and Brawer MK. Temporal trends in rates of prostate cancer: declining incidence of advanced stage disease, 1974 to 1994. J Urol 1997; 158: 1427-30.

[3] Mottet N, van den Bergh RCN, Briers E, Van den Broeck T, Cumberbatch MG, De Santis M, Fanti S, Fossati N, Gandaglia G, Gillessen S, Grivas N, Grummet J, Henry AM, van der Kwast TH, Lam TB, Lardas M, Liew M, Mason MD, Moris L, Oprea-Lager DE, van der Poel HG, Rouvière O, Schoots IG, Tilki D, Wiegel T, Willemse PM and Cornford P. EAU-EANM-ESTRO-ESUR-SIOG guidelines on prostate cancer-2020 update. Part 1: screening, diagnosis, and local treatment with curative intent. Eur Urol 2021; 79: 243-262.

[4] Freedland SJ, Humphreys EB, Mangold LA, Eisenberger M and Partin AW. Time to prostate specific antigen recurrence after radical prostatectomy and risk of prostate cancer specific mortality. J Urol 2006; 176: 1404-8.

[5] Van den Broeck T, van den Bergh RCN, Arfi N, Gross T, Moris L, Briers E, Cumberbatch M, De Santis M, Tilki D, Fanti S, Fossati N, Gillessen S, Grummet JP, Henry AM, Lardas M, Liew M, Rouvière O, Pecanka J, Mason MD, Schoots IG, van Der Kwast TH, van Der Poel HG, Wiegel T, Willemse PM, Yuan Y, Lam TB, Cornford P and Mottet N. Prognostic value of biochemical recurrence following treatment with curative intent for prostate cancer: a systematic review. Eur Urol 2019; 75: 967-987.

[6] Meng J, Lu X, Zhou Y, Zhang M, Gao L, Gao S, Yan F and Liang C. Characterization of the prognostic values and response to immunotherapy/chemotherapy of Krüppel-like factors in prostate cancer. J Cell Mol Med 2020; 24: 5797-5810.

[7] Gorgoulis V, Adams PD, Alimonti A, Bennett DC, Bischof O, Bishop C, Campisi J, Collado M, Evangelou K, Ferbeyre G, Gil J, Hara E, Krizhanovsky V, Jurk D, Maier AB, Narita M, Niedernhofer L, Passos JF, Robbins PD, Schmitt CA, Sedivy J, Vougas K, von Zglinicki T, Zhou D, Serrano M and Demaria M. Cellular senescence:

defining a path forward. Cell 2019; 179: 813-827.
[8] Sieben CJ, Sturmlechner I, van de Sluis B and van Deursen JM. Two-step senescence-focused cancer therapies. Trends Cell Biol 2018; 28: 723-737.
[9] Saleh T, Bloukh S, Carpenter VJ, Alwohoush E, Bakeer J, Darwish S, Azab B and Gewirtz DA. Therapy-induced senescence: an "old" friend becomes the enemy. Cancers (Basel) 2020; 12: 822.
[10] Lujambio A, Akkari L, Simon J, Grace D, Tschaharganeh DF, Bolden JE, Zhao Z, Thapar V, Joyce JA, Krizhanovsky V and Lowe SW. Non-cell-autonomous tumor suppression by p53. Cell 2013; 153: 449-60.
[11] Toso A, Revandkar A, Di Mitri D, Guccini I, Proietti M, Sarti M, Pinton S, Zhang J, Kalathur M, Civenni G, Jarrossay D, Montani E, Marini C, Garcia-Escudero R, Scanziani E, Grassi F, Pandolfi PP, Catapano CV and Alimonti A. Enhancing chemotherapy efficacy in pten-deficient prostate tumors by activating the senescence-associated antitumor immunity. Cell Rep 2014; 9: 75-89.
[12] Guccini I, Revandkar A, D'Ambrosio M, Colucci M, Pasquini E, Mosole S, Troiani M, Brina D, Sheibani-Tezerji R, Elia AR, Rinaldi A, Pernigoni N, Rüschoff JH, Dettwiler S, De Marzo AM, Antonarakis ES, Borrelli C, Moor AE, Garcia-Escudero R, Alajati A, Attanasio G, Losa M, Moch H, Wild P, Egger G and Alimonti A. Senescence reprogramming by TIMP1 deficiency promotes prostate cancer metastasis. Cancer Cell 2021; 39: 68-82, e9.
[13] Camphausen K, Moses MA, Beecken WD, Khan MK, Folkman J and O'Reilly MS. Radiation therapy to a primary tumor accelerates metastatic growth in mice. Cancer Res 2001; 61: 2207-11.
[14] Demaria M, O'Leary MN, Chang J, Shao L, Liu S, Alimirah F, Koenig K, Le C, Mitin N, Deal AM, Alston S, Academia EC, Kilmarx S, Valdovinos A, Wang B, de Bruin A, Kennedy BK, Melov S, Zhou D, Sharpless NE, Muss H and Campisi J. Cellular senescence promotes adverse effects of chemotherapy and cancer relapse. Cancer Discov 2017; 7: 165-176.
[15] Kim YH, Choi YW, Lee J, Soh EY, Kim JH and Park TJ. Senescent tumor cells lead the collective invasion in thyroid cancer. Nat Commun 2017; 8: 15208.
[16] Milanovic M, Fan DNY, Belenki D, Däbritz JHM, Zhao Z, Yu Y, Dörr JR, Dimitrova L, Lenze D, Monteiro Barbosa IA, Mendoza-Parra MA, Kanashova T, Metzner M, Pardon K, Reimann M, Trumpp A, Dörken B, Zuber J, Gronemeyer H, Hummel M, Dittmar G, Lee S and Schmitt CA. Senescence-associated reprogramming promotes cancer stemness. Nature 2018; 553: 96-100.
[17] Mortensen MM, Høyer S, Lynnerup AS, Ørntoft TF, Sørensen KD, Borre M and Dyrskjøt L. Expression profiling of prostate cancer tissue delineates genes associated with recurrence after prostatectomy. Sci Rep 2015; 5: 16018.
[18] Kuner R, Fälth M, Pressinotti NC, Brase JC, Puig SB, Metzger J, Gade S, Schäfer G, Bartsch G, Steiner E, Klocker H and Sültmann H. The maternal embryonic leucine zipper kinase (MELK) is upregulated in high-grade prostate cancer. J Mol Med (Berl) 2013; 91: 237-48.
[19] Penney KL, Sinnott JA, Tyekucheva S, Gerke T, Shui IM, Kraft P, Sesso HD, Freedman ML, Loda M, Mucci LA and Stampfer MJ. Association of prostate cancer risk variants with gene expression in normal and tumor tissue. Cancer Epidemiol Biomarkers Prev 2015; 24: 255-60.
[20] Jain S, Lyons CA, Walker SM, McQuaid S, Hynes SO, Mitchell DM, Pang B, Logan GE, McCavigan AM, O'Rourke D, McArt DG, McDade SS, Mills IG, Prise KM, Knight LA, Steele CJ, Medlow PW, Berge V, Katz B, Loblaw DA, Harkin DP, James JA, O'Sullivan JM, Kennedy RD and Waugh DJ. Validation of a metastatic assay using biopsies to improve risk stratification in patients with prostate cancer treated with radical radiation therapy. Ann Oncol 2018; 29: 215-222.
[21] Feng D, Shi X, Zhang F, Xiong Q, Wei Q and Yang L. Mitochondria dysfunction-mediated molecular subtypes and gene prognostic index for prostate cancer patients undergoing radical prostatectomy or radiotherapy. Front Oncol 2022; 12: 858479.
[22] Stelzer G, Rosen N, Plaschkes I, Zimmerman S, Twik M, Fishilevich S, Stein TI, Nudel R, Lieder I, Mazor Y, Kaplan S, Dahary D, Warshawsky D, Guan-Golan Y, Kohn A, Rappaport N, Safran M and Lancet D. The GeneCards suite: from gene data mining to disease genome sequence analyses. Curr Protoc Bioinformatics 2016; 54: 1.30.1-1.30.33.
[23] Kubisch R, Meissner L, Krebs S, Blum H, Günther M, Roidl A and Wagner E. A comprehensive gene expression analysis of resistance formation upon metronomic cyclophosphamide therapy. Transl Oncol 2013; 6: 1-9.
[24] Warde-Farley D, Donaldson SL, Comes O, Zuberi K, Badrawi R, Chao P, Franz M, Grouios C, Kazi F, Lopes CT, Maitland A, Mostafavi S, Montojo J, Shao Q, Wright G, Bader GD and Morris Q. The GeneMANIA prediction server: biological network integration for gene prioritization and predicting gene function. Nucleic Acids Res 2010; 38: W214-20.
[25] Han H, Cho JW, Lee S, Yun A, Kim H, Bae D, Yang S, Kim CY, Lee M, Kim E, Lee S, Kang B,

Jeong D, Kim Y, Jeon HN, Jung H, Nam S, Chung M, Kim JH and Lee I. TRRUST v2: an expanded reference database of human and mouse transcriptional regulatory interactions. Nucleic Acids Res 2018; 46: D380-D386.
[26] Paraskevopoulou MD, Vlachos IS, Karagkouni D, Georgakilas G, Kanellos I, Vergoulis T, Zagganas K, Tsanakas P, Floros E, Dalamagas T and Hatzigeorgiou AG. DIANA-LncBase v2: indexing microRNA targets on non-coding transcripts. Nucleic Acids Res 2016; 44: D231-8.
[27] Sticht C, De La Torre C, Parveen A and Gretz N. miRWalk: an online resource for prediction of microRNA binding sites. PLoS One 2018; 13: e0206239.
[28] Liu CJ, Hu FF, Xia MX, Han L, Zhang Q and Guo AY. GSCALite: a web server for gene set cancer analysis. Bioinformatics 2018; 34: 3771-3772.
[29] Mitsopoulos C, Di Micco P, Fernandez EV, Dolciami D, Holt E, Mica IL, Coker EA, Tym JE, Campbell J, Che KH, Ozer B, Kannas C, Antolin AA, Workman P and Al-Lazikani B. canSAR: update to the cancer translational research and drug discovery knowledgebase. Nucleic Acids Res 2021; 49: D1074-D1082.
[30] Liberzon A, Subramanian A, Pinchback R, Thorvaldsdóttir H, Tamayo P and Mesirov JP. Molecular signatures database (MSigDB) 3.0. Bioinformatics 2011; 27: 1739-40.
[31] Zhang Z, Zhang X and Huang A. Aggresome-autophagy associated gene HDAC6 is a potential biomarker in pan-cancer, especially in colon adenocarcinoma. Front Oncol 2021; 11: 718589.
[32] Finotello F, Mayer C, Plattner C, Laschober G, Rieder D, Hackl H, Krogsdam A, Loncova Z, Posch W, Wilflingseder D, Sopper S, Ijsselsteijn M, Brouwer TP, Johnson D, Xu Y, Wang Y, Sanders ME, Estrada MV, Ericsson-Gonzalez P, Charoentong P, Balko J, de Miranda NFDCC and Trajanoski Z. Molecular and pharmacological modulators of the tumor immune contexture revealed by deconvolution of RNA-seq data. Genome Med 2019; 11: 34.
[33] Yoshihara K, Shahmoradgoli M, Martínez E, Vegesna R, Kim H, Torres-Garcia W, Treviño V, Shen H, Laird PW, Levine DA, Carter SL, Getz G, Stemke-Hale K, Mills GB and Verhaak RG. Inferring tumour purity and stromal and immune cell admixture from expression data. Nat Commun 2013; 4: 2612.
[34] Zeng D, Ye Z, Shen R, Yu G, Wu J, Xiong Y, Zhou R, Qiu W, Huang N, Sun L, Li X, Bin J, Liao Y, Shi M and Liao W. IOBR: multi-omics immuno-oncology biological research to decode tumor microenvironment and signatures. Front Immunol 2021; 12: 687975.
[35] Shannon P, Markiel A, Ozier O, Baliga NS, Wang JT, Ramage D, Amin N, Schwikowski B and Ideker T. Cytoscape: a software environment for integrated models of biomolecular interaction networks. Genome Res 2003; 13: 2498-504.
[36] Hamdy FC, Donovan JL, Lane JA, Mason M, Metcalfe C, Holding P, Davis M, Peters TJ, Turner EL, Martin RM, Oxley J, Robinson M, Staffurth J, Walsh E, Bollina P, Catto J, Doble A, Doherty A, Gillatt D, Kockelbergh R, Kynaston H, Paul A, Powell P, Prescott S, Rosario DJ, Rowe E and Neal DE; ProtecT Study Group. 10-year outcomes after monitoring, surgery, or radiotherapy for localized prostate cancer. N Engl J Med 2016; 375: 1415-1424.
[37] Chang AJ, Autio KA, Roach M 3rd and Scher HI. High-risk prostate cancer-classification and therapy. Nat Rev Clin Oncol 2014; 11: 308-23.
[38] Van den Broeck T, van den Bergh RCN, Briers E, Cornford P, Cumberbatch M, Tilki D, De Santis M, Fanti S, Fossati N, Gillessen S, Grummet JP, Henry AM, Lardas M, Liew M, Mason M, Moris L, Schoots IG, van der Kwast T, van der Poel H, Wiegel T, Willemse PM, Rouvière O, Lam TB and Mottet N. Biochemical recurrence in prostate cancer: the European Association of Urology Prostate Cancer guidelines panel recommendations. Eur Urol Focus 2020; 6: 231-234.
[39] Becker DJ, Iyengar AD, Punekar SR, Ng J, Zaman A, Loeb S, Becker KD and Makarov D. Treatment of metastatic castration-resistant prostate cancer with abiraterone and enzalutamide despite PSA progression. Anticancer Res 2019; 39: 2467-2473.
[40] Campisi J. Cancer, aging and cellular senescence. Vivo 2000; 14: 183-8.
[41] Shay JW and Bacchetti S. A survey of telomerase activity in human cancer. Eur J Cancer 1997; 33: 787-91.
[42] Saleh T, Tyutyunyk-Massey L and Gewirtz DA. Tumor cell escape from therapy-induced senescence as a model of disease recurrence after dormancy. Cancer Res 2019; 79: 1044-6.
[43] Alotaibi M, Sharma K, Saleh T, Povirk LF, Hendrickson EA and Gewirtz DA. Radiosensitization by PARP inhibition in DNA repair proficient and deficient tumor cells: proliferative recovery in senescent cells. Radiat Res 2016; 185: 229-45.
[44] Achuthan S, Santhoshkumar TR, Prabhakar J, Nair SA and Pillai MR. Drug-induced senescence generates chemoresistant stemlike cells with low reactive oxygen species. J Biol Chem 2011; 286: 37813-29.
[45] Sabisz M and Skladanowski A. Cancer stem cells and escape from drug-induced premature senescence in human lung tumor cells: implications for drug resistance and in vitro

drug screening models. Cell Cycle 2009; 8: 3208-17.
[46] Wang Q, Wu PC, Dong DZ, Ivanova I, Chu E, Zeliadt S, Vesselle H and Wu DY. Polyploidy road to therapy-induced cellular senescence and escape. Int J Cancer 2013; 132: 1505-15.
[47] Kelly J, Ali Khan A, Yin J, Ferguson TA and Apte RS. Senescence regulates macrophage activation and angiogenic fate at sites of tissue injury in mice. J Clin Invest 2007; 117: 3421-6.
[48] Sagiv A and Krizhanovsky V. Immunosurveillance of senescent cells: the bright side of the senescence program. Biogerontology 2013; 14: 617-28.
[49] Coppé JP, Patil CK, Rodier F, Sun Y, Muñoz DP, Goldstein J, Nelson PS, Desprez PY and Campisi J. Senescence-associated secretory phenotypes reveal cell-nonautonomous functions of oncogenic RAS and the p53 tumor suppressor. PLoS Biol 2008; 6: 2853-68.
[50] Ohanna M, Cheli Y, Bonet C, Bonazzi VF, Allegra M, Giuliano S, Bille K, Bahadoran P, Giacchero D, Lacour JP, Boyle GM, Hayward NF, Bertolotto C and Ballotti R. Secretome from senescent melanoma engages the STAT3 pathway to favor reprogramming of naive melanoma towards a tumor-initiating cell phenotype. Oncotarget 2013; 4: 2212-24.
[51] Ohuchida K, Mizumoto K, Murakami M, Qian LW, Sato N, Nagai E, Matsumoto K, Nakamura T and Tanaka M. Radiation to stromal fibroblasts increases invasiveness of pancreatic cancer cells through tumor-stromal interactions. Cancer Res 2004; 64: 3215-22.
[52] Ortiz-Montero P, Londono-Vallejo A and Vernot JP. Senescence-associated IL-6 and IL-8 cytokines induce a self- and cross-reinforced senescence/inflammatory milieu strengthening tumorigenic capabilities in the MCF-7 breast cancer cell line. Cell Commun Signal 2017; 15: 17.
[53] Ewald J, Desotelle J, Almassi N and Jarrard D. Drug-induced senescence bystander proliferation in prostate cancer cells in vitro and in vivo. Br J Cancer 2008; 98: 1244-9.
[54] Capasso S, Alessio N, Squillaro T, Di Bernardo G, Melone MA, Cipollaro M, Peluso G and Galderisi U. Changes in autophagy, proteasome activity and metabolism to determine a specific signature for acute and chronic senescent mesenchymal stromal cells. Oncotarget 2015; 6: 39457-68.
[55] Özcan S, Alessio N, Acar MB, Mert E, Omerli F, Peluso G and Galderisi U. Unbiased analysis of senescence associated secretory phenotype (SASP) to identify common components following different genotoxic stresses. Aging (Albany NY) 2016; 8: 1316-29.
[56] Alessio N, Aprile D, Squillaro T, Di Bernardo G, Finicelli M, Melone MA, Peluso G and Galderisi U. The senescence-associated secretory phenotype (SASP) from mesenchymal stromal cells impairs growth of immortalized prostate cells but has no effect on metastatic prostatic cancer cells. Aging (Albany NY) 2019; 11: 5817-5828.
[57] Campisi J and d'Adda di Fagagna F. Cellular senescence: when bad things happen to good cells. Nat Rev Mol Cell Biol 2007; 8: 729-40.
[58] van Deursen JM. The role of senescent cells in ageing. Nature 2014; 509: 439-46.
[59] Tonnessen-Murray CA, Frey WD, Rao SG, Shahbandi A, Ungerleider NA, Olayiwola JO, Murray LB, Vinson BT, Chrisey DB, Lord CJ and Jackson JG. Chemotherapy-induced senescent cancer cells engulf other cells to enhance their survival. J Cell Biol 2019; 218: 3827-3844.
[60] Kyjacova L, Hubackova S, Krejcikova K, Strauss R, Hanzlikova H, Dzijak R, Imrichova T, Simova J, Reinis M, Bartek J and Hodny Z. Radiotherapy-induced plasticity of prostate cancer mobilizes stem-like non-adherent, Erk signaling-dependent cells. Cell Death Differ 2015; 22: 898-911.
[61] Hoey C, Ray J, Jeon J, Huang X, Taeb S, Ylanko J, Andrews DW, Boutros PC and Liu SK. miRNA-106a and prostate cancer radioresistance: a novel role for LITAF in ATM regulation. Mol Oncol 2018; 12: 1324-1341.
[62] Li M, Zhang W, Zhang S, Wang C and Lin Y. PART1 expression is associated with poor prognosis and tumor recurrence in stage I-III non-small cell lung cancer. J Cancer 2017; 8: 1795-1800.
[63] Lv Y, Wei W, Huang Z, Chen Z, Fang Y, Pan L, Han X and Xu Z. Long non-coding RNA expression profile can predict early recurrence in hepatocellular carcinoma after curative resection. Hepatol Res 2018; 48: 1140-1148.
[64] Ye J, Zhang J, Lv Y, Wei J, Shen X, Huang J, Wu S and Luo X. Integrated analysis of a competing endogenous RNA network reveals key long noncoding RNAs as potential prognostic biomarkers for hepatocellular carcinoma. J Cell Biochem 2019; 120: 13810-13825.
[65] Chang IW, Liu KW, Ragunanan M, He HL, Shiue YL and Yu SC. SERPINB5 expression: association with CCRT response and prognostic value in rectal cancer. Int J Med Sci 2018; 15: 376-384.
[66] Zhang P, Li X, He Q, Zhang L, Song K, Yang X, He Q, Wang Y, Hong X, Ma J and Liu N. TRIM21-SERPINB5 aids GMPS repression to protect nasopharyngeal carcinoma cells from radiation-induced apoptosis. J Biomed Sci 2020; 27: 30.

[67] Nelson G, Wordsworth J, Wang C, Jurk D, Lawless C, Martin-Ruiz C and von Zglinicki T. A senescent cell bystander effect: senescence-induced senescence. Aging Cell 2012; 11: 345-9.
[68] Mikuła-Pietrasik J, Sosińska P, Janus J, Rubiś B, Brewińska-Olchowik M, Piwocka K and Książek K. Bystander senescence in human peritoneal mesothelium and fibroblasts is related to thrombospondin-1-dependent activation of transforming growth factor-β1. Int J Biochem Cell Biol 2013; 45: 2087-96.
[69] Rhyu DY, Yang Y, Ha H, Lee GT, Song JS, Uh ST and Lee HB. Role of reactive oxygen species in TGF-beta1-induced mitogen-activated protein kinase activation and epithelial-mesenchymal transition in renal tubular epithelial cells. J Am Soc Nephrol 2005; 16: 667-75.
[70] Debacq-Chainiaux F, Borlon C, Pascal T, Royer V, Eliaers F, Ninane N, Carrard G, Friguet B, de Longueville F, Boffe S, Remacle J and Toussaint O. Repeated exposure of human skin fibroblasts to UVB at subcytotoxic level triggers premature senescence through the TGF-beta1 signaling pathway. J Cell Sci 2005; 118: 743-58.
[71] Kim KH, Park GT, Lim YB, Rue SW, Jung JC, Sonn JK, Bae YS, Park JW and Lee YS. Expression of connective tissue growth factor, a biomarker in senescence of human diploid fibroblasts, is up-regulated by a transforming growth factor-beta-mediated signaling pathway. Biochem Biophys Res Commun 2004; 318: 819-25.
[72] Chatterjee A, Kosmacek EA and Oberley-Deegan RE. MnTE-2-PyP treatment, or NOX4 inhibition, protects against radiation-induced damage in mouse primary prostate fibroblasts by inhibiting the TGF-beta 1 signaling pathway. Radiat Res 2017; 187: 367-81.
[73] Lu P, Weaver VM and Werb Z. The extracellular matrix: a dynamic niche in cancer progression. J Cell Biol 2012; 196: 395-406.
[74] Riegler J, Labyed Y, Rosenzweig S, Javinal V, Castiglioni A, Dominguez CX, Long JE, Li Q, Sandoval W, Junttila MR, Turley SJ, Schartner J and Carano RAD. Tumor elastography and its association with collagen and the tumor microenvironment. Clin Cancer Res 2018; 24: 4455-4467.
[75] Lichner Z, Ding Q, Samaan S, Saleh C, Nasser A, Al-Haddad S, Samuel JN, Fleshner NE, Stephan C, Jung K and Yousef GM. miRNAs dysregulated in association with Gleason grade regulate extracellular matrix, cytoskeleton and androgen receptor pathways. J Pathol 2015; 237: 226-37.
[76] Zhao SG, Lehrer J, Chang SL, Das R, Erho N, Liu Y, Sjöström M, Den RB, Freedland SJ, Klein EA, Karnes RJ, Schaeffer EM, Xu M, Speers C, Nguyen PL, Ross AE, Chan JM, Cooperberg MR, Carroll PR, Davicioni E, Fong L, Spratt DE and Feng FY. The immune landscape of prostate cancer and nomination of PD-L2 as a potential therapeutic target. J Natl Cancer Inst 2019; 111: 301-310.
[77] Zhu A, Hopkins KM, Friedman RA, Bernstock JD, Broustas CG and Lieberman HB. DNMT1 and DNMT3B regulate tumorigenicity of human prostate cancer cells by controlling RAD9 expression through targeted methylation. Carcinogenesis 2021; 42: 220-231.
[78] Tzelepi V, Logotheti S, Efstathiou E, Troncoso P, Aparicio A, Sakellakis M, Hoang A, Perimenis P, Melachrinou M, Logothetis C and Zolota V. Epigenetics and prostate cancer: defining the timing of DNA methyltransferase deregulation during prostate cancer progression. Pathology 2020; 52: 218-227.
[79] Zelic R, Fiano V, Ebot EM, Coseo Markt S, Grasso C, Trevisan M, De Marco L, Delsedime L, Zugna D, Mucci LA and Richiardi L. Single-nucleotide polymorphisms in DNMT3B gene and DNMT3B mRNA expression in association with prostate cancer mortality. Prostate Cancer Prostatic Dis 2019; 22: 284-291.
[80] Kim J and Bae JS. Tumor-associated macrophages and neutrophils in tumor microenvironment. Mediators Inflamm 2016; 2016: 6058147.
[81] Stein Y, Aloni-Grinstein R and Rotter V. Mutant p53-a potential player in shaping the tumor-stroma crosstalk. J Mol Cell Biol 2019; 11: 600-4.
[82] Hanahan D and Weinberg RA. Hallmarks of cancer: the next generation. Cell 2011; 144: 646-74.
[83] Murray PJ and Wynn TA. Protective and pathogenic functions of macrophage subsets. Nat Rev Immunol 2011; 11: 723-37.
[84] Sica A and Mantovani A. Macrophage plasticity and polarization: in vivo veritas. J Clin Invest 2012; 122: 787-95.
[85] Italiani P and Boraschi D. From monocytes to M1/M2 macrophages: phenotypical vs. functional differentiation. Front Immunol 2014; 5: 514.
[86] Di Mitri D, Mirenda M, Vasilevska J, Calcinotto A, Delaleu N, Revandkar A, Gil V, Boysen G, Losa M, Mosole S, Pasquini E, D'Antuono R, Masetti M, Zagato E, Chiorino G, Ostano P, Rinaldi A, Gnetti L, Graupera M, Martins Figueiredo Fonseca AR, Pereira Mestre R, Waugh D, Barry S, De Bono J and Alimonti A. Re-education of tumor-associated macrophages by CXCR2 blockade drives senescence and tumor inhibition in advanced prostate cancer. Cell Rep 2019; 28: 2156-2168, e5.

[87] Beatty GL, Torigian DA, Chiorean EG, Saboury B, Brothers A, Alavi A, Troxel AB, Sun W, Teitelbaum UR, Vonderheide RH and O'Dwyer PJ. A phase I study of an agonist CD40 monoclonal antibody (CP-870,893) in combination with gemcitabine in patients with advanced pancreatic ductal adenocarcinoma. Clin Cancer Res 2013; 19: 6286-95.

[88] Ries CH, Cannarile MA, Hoves S, Benz J, Wartha K, Runza V, Rey-Giraud F, Pradel LP, Feuerhake F, Klaman I, Jones T, Jucknischke U, Scheiblich S, Kaluza K, Gorr IH, Walz A, Abiraj K, Cassier PA, Sica A, Gomez-Roca C, de Visser KE, Italiano A, Le Tourneau C, Delord JP, Levitsky H, Blay JY and Rüttinger D. Targeting tumor-associated macrophages with anti-CSF-1R antibody reveals a strategy for cancer therapy. Cancer Cell 2014; 25: 846-59.

[89] Akdis M, Burgler S, Crameri R, Eiwegger T, Fujita H, Gomez E, Klunker S, Meyer N, O'Mahony L, Palomares O, Rhyner C, Ouaked N, Schaffartzik A, Van De Veen W, Zeller S, Zimmermann M and Akdis CA. Interleukins, from 1 to 37, and interferon-γ: receptors, functions, and roles in diseases. J Allergy Clin Immunol 2011; 127: 701-21, e1-70.

[90] Bromley SK, Mempel TR and Luster AD. Orchestrating the orchestrators: chemokines in control of T cell traffic. Nat Immunol 2008; 9: 970-80.

[91] Coppé JP, Desprez PY, Krtolica A and Campisi J. The senescence-associated secretory phenotype: the dark side of tumor suppression. Annu Rev Pathol 2010; 5: 99-118.

[92] Kang TW, Yevsa T, Woller N, Hoenicke L, Wuestefeld T, Dauch D, Hohmeyer A, Gereke M, Rudalska R, Potapova A, Iken M, Vucur M, Weiss S, Heikenwalder M, Khan S, Gil J, Bruder D, Manns M, Schirmacher P, Tacke F, Ott M, Luedde T, Longerich T, Kubicka S and Zender L. Senescence surveillance of pre-malignant hepatocytes limits liver cancer development. Nature 2011; 479: 547-51.

[93] Hamann A and Syrbe U. T-cell trafficking into sites of inflammation. Rheumatology (Oxford) 2000; 39: 696-9.

[94] Mao Y, Keller ET, Garfield DH, Shen K and Wang J. Stromal cells in tumor microenvironment and breast cancer. Cancer Metastasis Rev 2013; 32: 303-15.

[95] Wu J, Liang C, Chen M and Su W. Association between tumor-stroma ratio and prognosis in solid tumor patients: a systematic review and meta-analysis. Oncotarget 2016; 7: 68954-68965.

[96] Zhang Y, Nojima S, Nakayama H, Jin Y and Enza H. Characteristics of normal stromal components and their correlation with cancer occurrence in human prostate. Oncol Rep 2003; 10: 207-11.

[97] Barron DA and Rowley DR. The reactive stroma microenvironment and prostate cancer progression. Endocr Relat Cancer 2012; 19: R187-204.

[98] Dvorak HF. Tumors: wounds that do not heal. Similarities between tumor stroma generation and wound healing. N Engl J Med 1986; 315: 1650-9.

[99] Tuxhorn JA, Ayala GE, Smith MJ, Smith VC, Dang TD and Rowley DR. Reactive stroma in human prostate cancer: induction of myofibroblast phenotype and extracellular matrix remodeling. Clin Cancer Res 2002; 8: 2912-23.

[100] Saeter T, Vlatkovic L, Waaler G, Servoll E, Nesland JM, Axcrona K and Axcrona U. The prognostic value of reactive stroma on prostate needle biopsy: a population-based study. Prostate 2015; 75: 662-71.

[101] Billis A, Meirelles L, Freitas LL, Polidoro AS, Fernandes HA, Padilha MM, Magna LA, Reis LO and Ferreira U. Adenocarcinoma on needle prostatic biopsies: does reactive stroma predicts biochemical recurrence in patients following radical prostatectomy? Int Braz J Urol 2013; 39: 320-7.

[102] Harjunpää H and Guillerey C. TIGIT as an emerging immune checkpoint. Clin Exp Immunol 2020; 200: 108-119.